



Thermal, mechanical, and upconversion properties of Er³⁺/Yb³⁺ co-doped titanate glass prepared by levitation method

Xiuhong Pan^{a,*}, Jianding Yu^b, Yan Liu^a, Shinichi Yoda^b, Huimei Yu^a, Minghui Zhang^a, Fei Ai^a, Fei Jin^a, Weiqing Jin^a

^a State Key Laboratory of High Performance Ceramics and Superfine Microstructure, Shanghai Institute of Ceramics, Chinese Academy of Sciences, Shanghai 200050, China

^b Japan Aerospace Exploration Agency, ISS Science Project Office, Tsukuba 305-8505, Japan

ARTICLE INFO

Article history:

Received 6 January 2011

Received in revised form 18 April 2011

Accepted 19 April 2011

Available online 27 April 2011

Keywords:

Thermal stability

Vickers hardness

Upconversion

Titanate glass

Levitation method

ABSTRACT

A novel Er³⁺/Yb³⁺ co-doped titanate glass sphere with diameter of 3.5 mm has been successfully fabricated by levitation method. Its thermal stability, mechanical property and upconversion behavior were investigated. The glass transition temperature T_g , onset crystallization temperature T_c , and peak crystallization temperature T_p , are as high as 820, 895 and 902 °C, respectively. Its Vickers hardness is found to be up to 7.85 GPa. Intense green and red upconversion emissions were obtained in this glassy sample upon 980 nm excitation. The results illustrate good potential of this class of material for practical application in frequency upconversion device. In addition, it is found that heating treatment above T_p can reduce the efficiency of upconversion fluorescence as well as deteriorate the mechanical property, due to the occurrence of La₄Ti₉O₂₄ crystals.

© 2011 Elsevier B.V. All rights reserved.

1. Introduction

Recently, rare earth doped glasses are very attractive in efficient conversion of infrared radiation to visible light [1–4], because of several inherent advantages over their crystalline contenders. Among the glassy materials, halide (fluoride, etc.) glasses are notable due to their lower phonon energy, which can reduce the nonradiative loss caused by multiphonon relaxation and thus realize strong upconversion luminescence [5–7].

Unfortunately, halide glasses usually perform low mechanical property and low thermal stability. Therefore they are limited for practical utility. Oxide glasses, on the other hand, might be better for practical application because of their higher thermal stability, chemical durability and mechanical property. But in conventional oxide glasses like silicates, borates, phosphates etc. upconversion emissions are usually weak because they typically have phonon energy exceeding 1000 cm⁻¹, which can suppress the excited state lifetime of rare earth ions [8]. Therefore, it is necessary to explore new robust oxide glasses with low phonon energy as the host. Some recent attempt has been focused on the development of rare earth doped low phonon oxide glasses (like antimonite, bismuthate and germanate glasses) [9–12].

Titanium dioxide can be a good candidate for upconversion generation due to its low cutoff phonons of energy (~600–700 cm⁻¹) [13]. However, titanate melt is difficult to form bulk glass by traditional method. Upconversion luminescence has been reported only in TiO₂ powder [14] or titanate thin films [15,16]. In the past several years, some efforts were made for fabrication of bulk titanate glasses through levitation method [17–19]. And their dielectric and refractive behavior have been investigated [20–22]. But to the best of our knowledge, there is still no report on upconversion property of bulk titanate glass.

In this article, TiO₂–La₂O₃–ZrO₂ (TLZ) bulk glass incorporated with Er³⁺ and Yb³⁺ ions has been prepared by aerodynamic levitation method. This titanate glass is characterized by high mechanical property and good thermal stability. Specially, strong upconversion luminescence has been observed.

2. Experimental

The host composition (mol%) of the titanate glass is 78TiO₂–18La₂O₃–4ZrO₂. Erbium and ytterbium ions in the form of Er₂O₃ and Yb₂O₃ were added in. The concentrations of Er³⁺ and Yb³⁺ ions were fixed to be 0.4 mol% and 0.2 mol%, respectively. Raw materials with stoichiometric compositions were mixed and compressed into small rod. The rod was heated and melted by laser irradiation in an aerodynamic levitation furnace. After quenching at a cooling rate of about 300 °C/s, sphere sample with diameter of ~3.5 mm was obtained. The detail of levitation experiment has been reported in Ref. [20]. Then the sphere glass was polished to be a 2 mm thick wafer for further measurement and analysis. The structure of the sample was analyzed by X-ray diffraction (XRD). Differential thermal analysis (DTA) was carried out to characterize its thermal stability. Its mechanical property

* Corresponding author. Tel.: +86 21 5241 2508; fax: +86 21 5241 3903.
E-mail address: xhan@mail.sic.ac.cn (X. Pan).

was estimated by Vickers hardness testing which was performed on an Akashi (AVK-A) hardness tester with an applied load of 1 kg for 10 s.

Upconversion luminescence spectra were recorded by a spectrofluorometer (Fluorolog-3, Jobin Yvon, France) equipped with Hamamatsu R928 photomultiplier tube. A 980 nm continuous wave diode laser was used as the excitation source.

3. Results and discussion

3.1. Structure and thermal stability

The $\text{Er}^{3+}/\text{Yb}^{3+}$ co-doped TLZ sample prepared by levitation method is a sphere with diameter of about 3.5 mm. The upper curve in Fig. 1 shows the X-ray diffraction pattern of the as-prepared TLZ glass sample. Weak and broad diffraction bands are observed in this pattern. That means there are no crystals formed in the sample. The inset in Fig. 1 is a photo of the TLZ wafer with both surfaces being well polished. Obviously, the TLZ glass performs high transparency in the region of visible light.

DTA thermograms were recorded to investigate the thermal stability of $\text{Er}^{3+}/\text{Yb}^{3+}$ co-doped TLZ glass. Fig. 2 shows the DTA curve at a heating rate of $10^\circ\text{C}/\text{min}$. This curve has a single glass transition and a single crystallization peak. The value of glass transition temperature T_g , onset crystallization temperature T_c , and peak crystallization temperature T_p , are about 820, 895 and 902°C , respectively. Noted that the T_p of present TLZ glass is much higher than that of fluoride or oxy-fluoride glass, which is usually lower than 400°C [23,24]. This hints that the TLZ glass has a better thermal stability against high temperature. Therefore, the upconversion

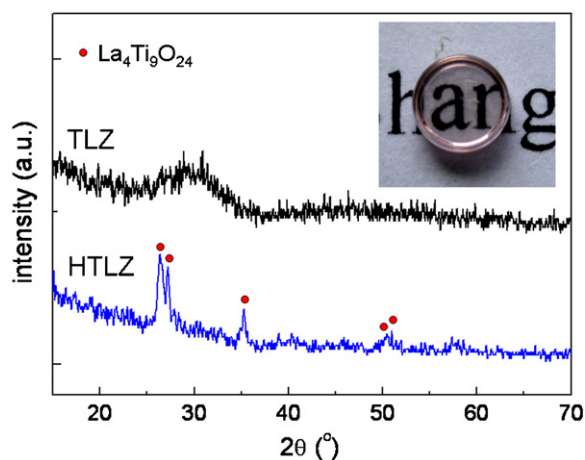


Fig. 1. X-ray patterns for the $\text{Er}^{3+}/\text{Yb}^{3+}$ co-doped TLZ and HTLZ samples. Inset shows the photo of the polished TLZ glass wafer.

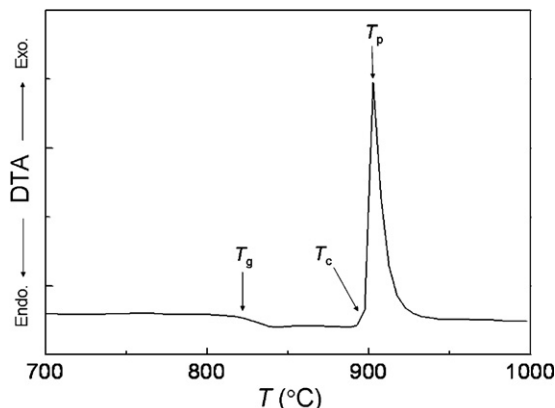


Fig. 2. DTA traces of TLZ glass sample with heating rate of $10^\circ\text{C}/\text{min}$.

devices based on this TLZ glass might be used for technological application more widely. Furthermore, the value of $\Delta T = T_c - T_g$, which is often an important parameter to characterize the glass forming ability [25] has also been calculated. The calculated ΔT of present TLZ glass is 75°C . This value is much lower than those of most traditional oxide glasses such as silicate or borate glass systems [26,27], and even lower than those of some heavy metal oxide glasses [28,29]. The result indicates a comparatively poor glass forming ability of the TLZ glass. This makes it difficult to obtain bulk titanate glass by traditional melt-quenching method. And it is the reason why levitation method must be introduced for titanate glass fabrication in present experiment.

3.2. Mechanical property

Vickers hardness was measured to evaluate the mechanical property of the $\text{Er}^{3+}/\text{Yb}^{3+}$ co-doped TLZ glass. The Vickers hardness was determined by using a micro-hardness tester equipped with a Vickers indenter. The indentation was examined by an optical microscopy. The surface morphology of the polished sample can also be observed by this microscopy. In order to estimate the mechanical property upon high temperature more deeply, the hardness of the heat-treated TLZ sample (HTLZ) was also investigated. The TLZ glass was heated in air for 10 s at 950°C , which is higher than T_p , and then HTLZ glass–ceramic is obtained.

Fig. 3(a) and (b) shows the typical microscopic images of the Vickers indentations for TLZ glass and HTLZ glass–ceramic, respectively. The shapes of the two indentations are similar and there are no significant shear bands observed for both TLZ and HTLZ samples. However, significant micro-cracks emanating from all the corners of the indentations can be noticed in both cases. It is obvious that the length of the crack in HTLZ sample is longer than that in the TLZ sample, indicating a deterioration of mechanical property due to heat treatment.

Quantitative value of Vickers hardness was averaged from three data points by the following standard formula: $H_v = 1.854P/d^2$ [30]. Here, H_v is the Vickers hardness, P is the applied load, and d is the mean length of the two diagonal lines of the indentation. The measured value of Vickers hardness is 7.85 GPa for the TLZ glass, which is much higher than that of ordinary fluoride glass (~ 2.0 GPa) [31]. This suggests a potential application for industrial device preparation based on present $\text{Er}^{3+}/\text{Yb}^{3+}$ co-doped titanate glass. However, the value of Vickers hardness for the HTLZ glass–ceramic has a little drop, which is about 7.56 GPa.

Furthermore, information of microstructure of the samples can also be obtained from Fig. 3. For the TLZ glass sample, there are no grains observed (Fig. 3(a)). However, for the HTLZ glass–ceramic sample, numerous grains with size of several microns are obvious (Fig. 3(b)). The X-ray diffraction pattern for the HTLZ sample is also shown in Fig. 1 by the bottom curve. Analysis of this X-ray diffraction pattern suggests that the grains in the HTLZ glass–ceramic are mainly crystallites of $\text{La}_4\text{Ti}_9\text{O}_{24}$.

3.3. Upconversion luminescence spectra

The upconversion emission spectrum (400–750 nm) of $\text{Er}^{3+}/\text{Yb}^{3+}$ co-doped TLZ glass has been recorded using 980 nm excitation as shown by the solid line in Fig. 4. There are totally three intense light emission bands centered at 530, 546 and 672 nm which are attributed to the Er^{3+} : ${}^2H_{11/2} \rightarrow {}^4I_{15/2}$, ${}^4S_{3/2} \rightarrow {}^4I_{15/2}$, and ${}^4F_{9/2} \rightarrow {}^4I_{15/2}$ transitions, respectively. It is apparent that the green emission at 546 nm has the highest peak intensity. The intensity of red emission at 672 nm is much weaker than that of green emission at 546 nm, but is almost the same as that of the green emission at 530 nm. It should be noted that the upconversion process in TLZ glass is so efficient that the green emission can be seen by naked

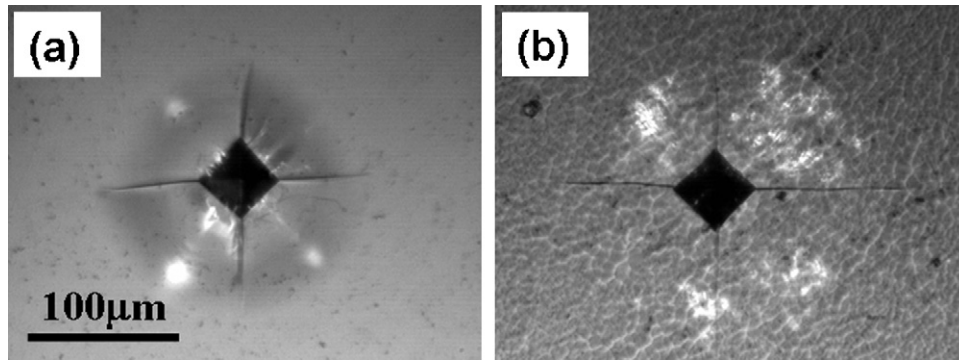


Fig. 3. Optical micrographs of Vickers indentations under 1 kg load in TLZ glass (a) and HTLZ glass-ceramic (b).

eyes with pump power as low as a several milliwatts. The inserted photo in Fig. 4 shows the fluorescent emission of the TLZ glass with pump power of 10 mW.

To understand the upconversion mechanism in $\text{Er}^{3+}/\text{Yb}^{3+}$ co-doped TLZ glass, the pump laser power dependence of the fluorescent radiation was investigated. In frequency upconversion process, the upconversion emission intensity I increases with pump power by the following relation: $I \propto P^n$, where I is the fluorescent intensity, P is the pump laser power, and n is the number of pump photons absorbed per upconverted photon emitted. The plot of $\log I$ versus $\log P$ yields a straight line with slope n at 980 nm excitation. The inset curve in Fig. 4 shows such a plot for the 530, 546 and 672 nm emissions in $\text{Er}^{3+}/\text{Yb}^{3+}$ co-doped TLZ glass. Values of 1.98, 1.88 and 1.77 are obtained for n corresponding to the 530, 546 and 672 nm emission bands, respectively. The results indicate that two photons are involved for both green and red upconversion processes in $\text{Er}^{3+}/\text{Yb}^{3+}$ co-doped TLZ glass.

The upconversion emission spectrum of HTLZ glass-ceramic is demonstrated by the dashed line in Fig. 4. Lower intensities are obtained for all upconversion emission bands in HTLZ glass-ceramic than those in TLZ glass. This can be well interpreted by taking into account of the effect of grain boundaries. The size of $\text{La}_4\text{Ti}_9\text{O}_{24}$ crystals in present HTLZ sample is up to several microns (Fig. 3(b)), which is large enough to induce dispersion in light transmission due to the significant grain boundaries [32]. As a result, the sample becomes opaque, and the upconversion emission intensity is decreased.

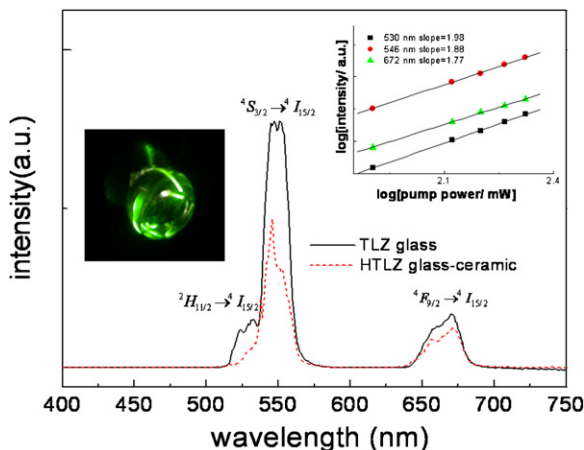


Fig. 4. Upconversion emission spectra of $\text{Er}^{3+}/\text{Yb}^{3+}$ co-doped TLZ glass (solid line) and HTLZ glass-ceramic (dashed line) upon excitation at 980 nm. Inset photo: fluorescence of TLZ glass under 10 mW pump power. Inset curve in the right shows the dependence of upconversion fluorescence intensity on excitation power.

What is more interesting is the sharpening of upconverted emission peaks for green lights in HTLZ glass-ceramic. It is clear that the green emissions at 530 and 546 nm have significant shoulder peaks at 524 and 554 nm, respectively, for the TLZ glass as shown by the solid line in Fig. 4. They are possibly due to the energy level splitting of $^2H_{11/2}$ and $^4S_{3/2}$ levels, respectively [33]. However, these shoulder peaks have been reduced in the HTLZ glass-ceramic. Consequently, the corresponding emission bands become sharper as indicated by the dashed line in Fig. 4.

4. Conclusions

In summary, $\text{Er}^{3+}/\text{Yb}^{3+}$ co-doped $\text{TiO}_2\text{-La}_2\text{O}_3\text{-ZrO}_2$ glass has been prepared by levitation method. This titanate glass presents high transparency, good thermal stability, and high mechanical property. Intense emission bands centered at 530, 546 and 672 nm are observed upon 980 nm excitation, corresponding to the Er^{3+} transitions $^2H_{11/2} \rightarrow ^4I_{15/2}$, $^4S_{3/2} \rightarrow ^4I_{15/2}$, and $^4F_{9/2} \rightarrow ^4I_{15/2}$ respectively. Two-photon processes are found responsible for all these upconversion emissions. When the glass is heated above its crystallization temperature, both the upconversion efficiency and the Vickers hardness are reduced.

Acknowledgements

This work was performed under the Projects supported by the Fund of the National Natural Science Foundation of China (51072209, 50802105), Project supported by the Shanghai Committee of Science and Technology, China (09JC1415300), and Project supported by Innovation Fund of Shanghai Institute of Ceramics, CAS (Y17ZC11601G).

References

- [1] R.K. Verma, D.K. Rai, S.B. Rai, J. Alloys Compd. 509 (2011) 5591–5595.
- [2] J. Ding, Q. Zhang, J. Cheng, X. Liu, G. Lin, J. Qiu, D. Chen, J. Alloys Compd. 495 (2010) 205–208.
- [3] F.A. Bomfim, J.R. Martinelli, L.R.P. Kassab, T.A.A. Assumpção, C.B. de Araujo, J. Non-Cryst. Solids 356 (2010) 2598–2601.
- [4] T. Som, B. Karmakar, Opt. Mater. 31 (2009) 609–618.
- [5] X. Qiao, X. Fan, Z. Xue, X. Xu, Q. Luo, J. Alloys Compd. 509 (2011) 4714–4721.
- [6] L. Feng, B. Lai, J. Wang, G. Du, Q. Su, J. Lumin. 130 (2010) 2418–2423.
- [7] P. Haro-González, I.R. Martín, N.E. Capuj, F. Lahoz, Opt. Mater. 32 (2010) 1349–1351.
- [8] G.A. Kumar, A. Martinez, E. Mejia, J.G. Eden, J. Alloys Compd. 365 (2004) 117–120.
- [9] J. Jakutis, L. Gomes, C.T. Amancio, L.R.P. Kassab, J.R. Martinelli, N.U. Wetter, Opt. Mater. 33 (2010) 107–111.
- [10] K. Li, H. Fan, G. Zhang, G. Bai, S. Fan, J. Zhang, L. Hu, J. Alloys Compd. 509 (2011) 3070–3073.
- [11] X.P. Jiang, Z.M. Yang, T. Liu, S.H. Xu, J. Appl. Phys. 105 (2009) 103113.
- [12] R. Xu, Y. Tian, M. Wang, L. Hu, J. Zhang, Opt. Mater. 33 (2011) 299–302.
- [13] T. Mazza, E. Barborini, P. Piseri, P. Milani, D. Cattaneo, A. Li Bassi, C.E. Bottani, C. Ducati, Phys. Rev. B 75 (2007) 045416.
- [14] S. Jeon, P.V. Braun, Chem. Mater. 15 (2003) 1256–1263.

- [15] I.K. Battisha, *J. Non-Cryst. Solids* 353 (2007) 1748–1754.
- [16] T. Ji, Y. Liu, H. Zhao, H. Du, J. Sun, G. Ge, *J. Solid State Chem.* 183 (2010) 584–589.
- [17] J. Yu, S. Kohara, K. Itoh, S. Nozawa, S. Miyoshi, Y. Arai, A. Masuno, H. Taniguchi, M. Itoh, M. Takata, T. Fukunaga, S. Koshihara, Y. Kuroiwa, S. Yoda, *Chem. Mater.* 21 (2009) 259–263.
- [18] J. Yu, P. Paradis, T. Ishikawa, S. Yoda, I. Miura, Y. Shan, *J. Cryst. Growth* 273 (2005) 515–519.
- [19] H. Taniguchi, J. Yu, Y. Arai, D. Fu, T. Yagi, M. Itoh, *Mater. Sci. Eng. B* 148 (2008) 48–52.
- [20] J. Yu, Y. Arai, T. Masaki, T. Ishikawa, S. Yoda, S. Kohara, H. Taniguchi, M. Itoh, Y. Kuroiwa, *Chem. Mater.* 18 (2006) 2169–2173.
- [21] Y. Arai, K. Itoh, S. Kohara, J. Yu, *J. Appl. Phys.* 103 (2008) 094905.
- [22] A. Masuno, H. Inoue, J. Yu, Y. Arai, *J. Appl. Phys.* 108 (2010) 063520.
- [23] P. Babu, H.J. Seo, C.R. Kesavulu, K.H. Jang, C.K. Jayasankar, *J. Lumin.* 129 (2009) 444–448.
- [24] C. Koepke, D. Piatkowski, K. Wisniewski, M. Naftaly, *J. Non-Cryst. Solids* 356 (2010) 435–440.
- [25] A. Dahshan, *J. Non-Cryst. Solids* 354 (2008) 3034–3039.
- [26] S.A.M. Abdel-Hameed, A.A. El-kheshen, *Ceram. Int.* 29 (2003) 265–269.
- [27] Y. Yang, Z. Yang, B. Chen, P. Li, X. Li, Q. Guo, *J. Alloys Compd.* 479 (2009) 883–887.
- [28] T. Xu, X. Zhang, S. Dai, Q. Nie, X. Shen, X. Zhang, *Phys. B* 389 (2007) 242–247.
- [29] S. Simon, V. Simon, *Mater. Lett.* 58 (2004) 3778–3781.
- [30] M.T. Lin, D.Y. Jiang, L. Li, Z.L. Lu, T.R. Lai, J.L. Shi, *Mater. Sci. Eng. A* 351 (2003) 9–14.
- [31] A. Delben, Y. Messaddeq, M.D. Caridade, M.A. Aegerter, J.A. Eiras, *J. Non-Cryst. Solids* 161 (1993) 165–168.
- [32] Z. Duan, J. Zhang, D. He, H. Sun, L. Hu, *Mater. Chem. Phys.* 100 (2006) 400–403.
- [33] J. Zhang, S. Dai, G. Wang, L. Zhang, H. Sun, L. Hu, *Phys. Lett. A* 345 (2005) 409–414.